

Transverse Momentum Distributions in B-Decays

U. Aglietti^{*)}

Theoretical Physics Division, CERN
CH - 1211 Geneva 23

R. Sghedoni^{**)} and L. Trentadue^{***)}

Dipartimento di Fisica, Università di Parma
and
Gruppo Collegato INFN, Viale delle Scienze 7a, 43100 Parma

We consider transverse momentum distributions in B -decays. The $\mathcal{O}(\alpha_S)$ coefficients for soft and collinear logarithms are computed to next-to-leading accuracy. Resummation of large logarithmic contributions is performed in impact parameter space within the general formalism for transverse momentum distributions. It is shown that the shape-function approach as used for the threshold distribution case cannot be extended to the transverse momentum one.

^{*)} On leave of absence from Dipartimento di Fisica, Università di Roma I, Piazzale Aldo Moro 2, 00185 Roma, Italy. E-mail address: ugo.aglietti@cern.ch.

^{**)} E-mail address: roberto.sghedoni@fis.unipr.it

^{***)} E-mail address: luca.trentadue@fis.unipr.it

1 Introduction

In this note we discuss transverse momentum distributions in heavy flavour decays. As may be easily recognized, the structure of the expressions reflects the analogous case of the energy-energy correlations or shape variables in e^+e^- annihilation, i.e. it involves a coefficient function, a universal function f containing the logarithmic contributions and a remainder function. This structure shows, on the other hand, the general form common to all the reactions such as Drell-Yan (DY), Deep Inelastic Scattering (DIS), Jet Shape variables, etc., once the large logarithmic contributions are separately resummed in the function f .

The purpose of computing the set of perturbative contributions for the heavy quark decay case is introduced in this paper together with some preliminary results. We compute the next-to-leading order (NLO) coefficient B_1 describing single-logarithmic effects, which, together with the universal A_1 and A_2 coefficients, determines the function f to NLO accuracy.

We outline here the peculiar phenomenological content of the transverse momentum distribution as making, for several reasons, a stand-alone case in heavy flavour physics.

The main phenomenological application of our work involves the spectrum of transverse momenta of the produced hadrons, with respect to the photon direction, in the reaction $b \rightarrow s\gamma$. This process appears to be very clean because, in the rest frame of the B -meson, the photon momentum unambiguously fixes the reference direction for transverse hadron momenta.

The final goal of our study is a comparison of the complete NLO perturbative distribution with equally accurate experimental data. Such a comparison should allow the extraction of the non-perturbative component in the process i.e. the Fermi motion effects of the b -quark inside the B -meson and the final-state hadronization of the strange quark. The information about non-perturbative dynamics obtained with p_\perp distributions is complementary to the one obtained with the well-studied threshold distributions. Roughly speaking, transverse momentum distributions are sensitive to the motion of the heavy quark in the plane orthogonal to the decay axis, while threshold distributions are sensitive to the motion along the decay axis. This topic deserves some attention since, as well known, the transverse momentum distributions of heavy flavours in hadronic processes are presently poorly understood.

The paper is organized as follows. In sec.2 we present our result on transverse momentum distributions. In sec.3 we summarize the main results on threshold distributions. In sec.4 we discuss the results and we compare the two different distributions. Finally, sec.5 contains the conclusions together with an outlook at future developments.

2 Transverse momentum distribution

As anticipated in the introduction, let us consider the distribution of relative transverse momenta between a strange hadron h_s and the photon in radiative B decays:

$$B \rightarrow h_s + X + \gamma, \tag{1}$$

In practice, we expect h_s to be a meson such as a K , a K^* , etc.. Without any generality loss, we can take the B -meson at rest and the photon flying along the plus direction ($+z$ axis); the relative transverse momentum then coincides with the projection of the h_s momentum in the $x - y$ plane. In general, we may identify three different mechanisms in transverse momentum dynamics:

1. *soft-gluon emission*. The elementary process in (1) is:

$$b \rightarrow s + \widehat{X} + \gamma. \tag{2}$$

Non-vanishing transverse momenta

$$\mathbf{p}_p \neq \mathbf{0} \quad (3)$$

are generated by soft-gluon emission¹;

2. *Fermi-motion*. The beauty quark and the light valence quark in the B -meson exchange soft momenta with each other. This implies that, before decay (2) occurs, the b quark has a non-zero transverse momentum

$$\mathbf{p}_f \sim \Lambda \quad (4)$$

where Λ is the QCD scale.

3. *final-state hadronization*. The strange quark emitted in the hard process fragments into the final hadron h_s ,

$$s \rightarrow h_s + (\text{anything}). \quad (5)$$

Since the latter is a soft process, this implies a change in the transverse momentum of the strange system by a quantity

$$\mathbf{p}_h \sim \Lambda. \quad (6)$$

The total transverse momentum of h_s is then

$$\mathbf{p} = \mathbf{p}_p + \mathbf{p}_f + \mathbf{p}_h. \quad (7)$$

Let us observe that Fermi motion and hadronization effects are of the same order and cannot therefore be separated from each other. As we are going to show later, the situation is instead different in threshold distributions. According to the above estimates, if we take

$$|\mathbf{p}| \gg \Lambda, \quad (8)$$

we have that the non-perturbative effects described in 2. and 3. are negligible, so that

$$\mathbf{p} \simeq \mathbf{p}_p, \quad (9)$$

and a (resummed) perturbative computation controls the distribution. The transverse momentum distribution in impact parameter space b [1, 2] has the characteristic form [3]–[6]:

$$\frac{1}{\Gamma_B} \frac{d\Gamma}{db} = C(\alpha_S) f(b; \alpha_S) + R(b; \alpha_S). \quad (10)$$

Γ_B is the Born width and is given by:

$$\Gamma_B \simeq \frac{\alpha_{em}}{\pi} \frac{G_F m_b^3 m_{b,MS}^2(m_b) |V_{tb} V_{ts}^*|^2}{32\pi^3} C_7^2(m_B), \quad (11)$$

where we consider only the leading operator O_7 in the effective $b \rightarrow s\gamma$ hamiltonian [7].

The coefficient function $C(\alpha_S)$ is process-dependent and short-distance dominated and has an expansion in powers of α_S of the form:

$$C(\alpha_S) = 1 + \frac{C_F \alpha_S}{\pi} c + \left(\frac{\alpha_S}{\pi}\right)^2 c' + \dots \quad (12)$$

¹Transverse momenta are generally denoted with boldface symbols.

where $C_F = (N_c^2 - 1) / (2N_c) = 4/3$, $\alpha_S \equiv \alpha_S(Q^2)$ and $Q = m_B$ is the hard scale. The remainder function R is process-dependent and has an expansion starting at order α_S of the form

$$R(b; \alpha_S) = \frac{C_F \alpha_S}{\pi} r(b) + \left(\frac{\alpha_S}{\pi}\right)^2 r'(b) + \dots \quad (13)$$

R vanishes in the limit of a large impact parameter:

$$R(b; \alpha_S) \rightarrow 0 \quad \text{for } b \rightarrow \infty, \quad (14)$$

implying that it is short-distance dominated.

The function $f(b; \alpha_S)$ contains the large logarithmic contributions in a resummed form and can be written as the exponential of a series of functions [4]:

$$f(b; \alpha_S) = \exp [L g_1(\beta_0 \alpha_S L) + g_2(\beta_0 \alpha_S L) + \alpha_S g_3(\beta_0 \alpha_S L) + \dots], \quad (15)$$

where

$$L \equiv \log \frac{Q^2 b^2}{b_0^2} \quad (16)$$

and $b_0 \equiv 2 \exp[-\gamma_E] \simeq 1.12$ with $\gamma_E \simeq 0.577$ the Euler constant. Our computation of the functions g_1 and g_2 gives:

$$g_1(\omega) = \frac{A_1}{2\beta_0} \frac{1}{\omega} [\log(1 - \omega) + \omega], \quad (17)$$

$$g_2(\omega) = -\frac{A_2}{2\beta_0^2} \left[\frac{\omega}{1 - \omega} + \log(1 - \omega) \right] + \frac{A_1 \beta_1}{2\beta_0^3} \left[\frac{\log(1 - \omega)}{1 - \omega} + \frac{\omega}{1 - \omega} + \frac{1}{2} \log^2(1 - \omega) \right] + \frac{B_1}{\beta_0} \log(1 - \omega), \quad (18)$$

where

$$A_1 = \frac{C_F}{\pi} \quad \text{and} \quad A_2 = \frac{C_F}{\pi^2} \left[C_A \left(\frac{67}{36} - \frac{\pi^2}{12} \right) - \frac{5}{9} n_f T_R \right]. \quad (19)$$

The above value of A_2 is in the \overline{MS} scheme for the coupling constant [2]. As usual, $C_A = N_c = 3$, $T_R = 1/2$ and $n_F = 3$ is the number of active quark flavours. The first two coefficients of the β -function are:

$$\beta_0 = \frac{11C_A - 2n_F}{12\pi} = \frac{33 - 2n_F}{12\pi}, \quad \beta_1 = \frac{17C_A^2 - 5C_A n_F - 3C_F n_F}{24\pi^2} = \frac{153 - 19n_F}{24\pi^2}. \quad (20)$$

A complete NLO analysis requires also the knowledge of the coefficient function c and of the remainder function $r(b)$ of order α_S , which at present are unknown. Their computation is in progress and will be presented in a forthcoming publication.

Denoting by S_1 the soft contribution at one loop and by C_1 the collinear one in the notation of ref. [8],

$$S_1 = -\frac{C_F}{\pi}, \quad C_1 = -\frac{3}{4} \frac{C_F}{\pi}, \quad (21)$$

the next-to-leading coefficient B_1 is given by

$$B_1 = \frac{S_1}{2} + C_1 = -\frac{5}{4} \frac{C_F}{\pi}. \quad (22)$$

In usual hard processes, such as DIS or DY, $S_1 = 0$ so that $B_1 = C_1$. In our case, single logarithmic effects are more pronounced because this coefficient is almost a factor of 2 larger.

The expansion to order α_S^2 of the exponent reads:

$$\log f(b; \alpha_S) = -\frac{1}{4} A_1 \alpha_S L^2 - B_1 \alpha_S L - \frac{1}{6} A_1 \beta_0 \alpha_S^2 L^3 - \frac{1}{4} A_2 \alpha_S^2 L^2 - \frac{1}{2} B_1 \beta_0 \alpha_S^2 L^2. \quad (23)$$

Let us note that a *single* constant B_1 controls the single-logarithmic effects in any order. The physical reason is that a soft gluon and a collinear one with the same transverse momenta are emitted with the same effective coupling $\alpha_S(k_\perp^2)$ [9]. This is to be contrasted with the threshold case (see next section). The function $f(b, \alpha_S)$ is plotted in fig. 1.

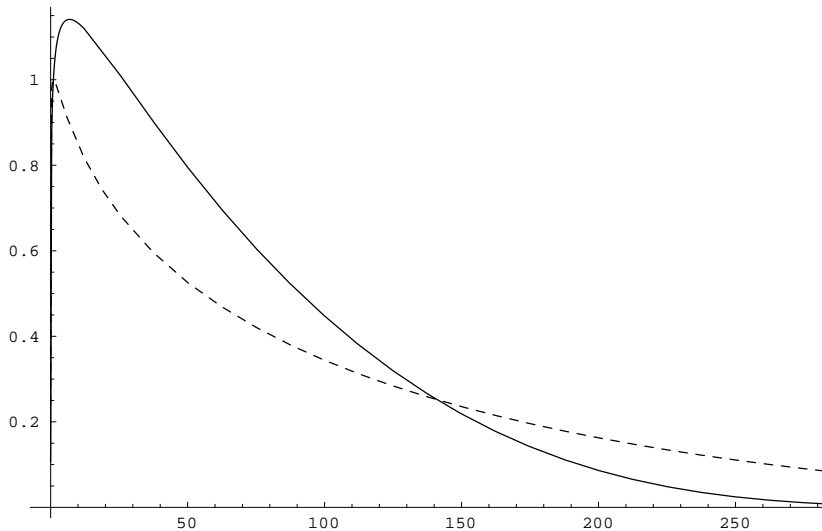


Fig. 1: Plot of the function $f(b)$ in the variable $y = Q^2 b^2 / b_0^2$ ($\alpha_S = 0.22$). Solid line: NLO; dotted line: LO.

The resummed distribution (10) becomes singular when

$$\omega \rightarrow 1^- \quad (24)$$

Since

$$\omega = \beta_0 \alpha_S L \approx \frac{\log Q^2 b^2}{\log Q^2 / \Lambda^2}, \quad (25)$$

the singularity occurs when the transverse strange momentum becomes as small as the hadronic scale,

$$p_\perp \approx \frac{1}{b} \approx \Lambda. \quad (26)$$

The singularity (24) is produced by the infrared pole in the running coupling and signals an intrinsic limitation of resummed perturbation theory, in agreement with previous qualitative analysis. Let us note that the function g_2 has basically a pole singularity in the limit (24), while g_1 has only a softer, logarithmic, singularity.

3 Threshold distribution

In this section we recall the main results on threshold distributions. The distribution in Mellin space — the N -moment of the rate — has a similar representation to (10) [3]–[5],

$$\frac{1}{\Gamma_B} \Gamma_N = \mathcal{C}(\alpha_S) f_N(\alpha_S) + R_N(\alpha_S), \quad (27)$$

where now the large logarithm contains the N -variable:

$$L \equiv \log \frac{N}{N_0} \quad (\text{threshold case}), \quad (28)$$

with $N_0 \equiv \exp[-\gamma_E]$. The functions g_i in the exponent are different with respect to the ones in the p_\perp case and the leading and next-to-leading ones read [10, 11]:

$$\begin{aligned} g_1(\lambda) &= -\frac{A_1}{2\beta_0} \frac{1}{\lambda} [(1-2\lambda)\log(1-2\lambda) - 2(1-\lambda)\log(1-\lambda)], \\ g_2(\lambda) &= \frac{\beta_0 A_2 - \beta_1 A_1}{2\beta_0^3} [\log(1-2\lambda) - 2\log(1-\lambda)] - \frac{\beta_1 A_1}{4\beta_0^3} [\log^2(1-2\lambda) - 2\log^2(1-\lambda)] + \\ &\quad + \frac{S_1}{2\beta_0} \log(1-2\lambda) + \frac{C_1}{\beta_0} \log(1-\lambda). \end{aligned} \quad (29)$$

The expansion to order α_S^2 of the exponent reads:

$$\log f_N = -\frac{1}{2} A_1 \alpha_S L^2 - \alpha_S (S_1 + C_1) L - \frac{1}{2} A_1 \beta_0 \alpha_S^2 L^3 - \frac{1}{2} A_2 \alpha_S^2 L^2 - \left(S_1 + \frac{1}{2} C_1 \right) \beta_0 \alpha_S^2 L^2. \quad (30)$$

Let us comment on the above results. The single-logarithmic effects at one loop are controlled by the constant

$$S_1 + C_1 = -\frac{7}{4} \frac{C_F}{\pi}, \quad (31)$$

i.e. by the sum of the soft and the collinear coefficients, which is different from the p_\perp -case (cf. eqs. (22) and (23)). At two-loop they are instead controlled by a different constant,

$$S_1 + \frac{1}{2} C_1 = -\frac{11}{8} \frac{C_F}{\pi}. \quad (32)$$

The soft and the collinear terms begin to differentiate at this order and the soft one has a two times larger coefficient. Contrary to the p_\perp case, two different constants are needed to describe the single logarithmic effects. The dynamical difference between soft and collinear terms is that, for a fixed jet mass, the transverse momentum of a soft gluon is substantially smaller than that of a collinear gluon [9, 12, 8, 11].

The functions g_1 and g_2 in (29) — and therefore also the resummed distribution — have two different singularities [11, 14, 15, 8]:

i) the first one occurs when

$$\frac{1}{2} = \lambda \approx \frac{\log Q^2/m^2}{\log Q^2/\Lambda^2}, \quad (33)$$

or, equivalently, when

$$m^2 \approx \Lambda Q, \quad (34)$$

where m is the mass of the final hadronic jet $s + \widehat{X}$. In the last member of (33), we have used the approximation $N \approx Q^2/m^2$ [16]. The singularity (33) signals the occurrence of non-perturbative effects in region (34) — to be identified with the well-known Fermi motion [17]; it is related to soft-gluon effects — i.e. to the terms proportional to A_1 , S_1 and A_2 — and not to collinear ones — the term proportional to C_1 . Fermi-motion effects are therefore controlled by soft and not by collinear dynamics. This fact allows a factorisation of Fermi-motion effects by means of a function taking into account soft dynamics only, the well-known shape function² [18]. In this region, initial bound state effects become relevant while final-state binding effects can be neglected [19, 8, 11].

²The shape function is also called structure function of the heavy flavours.

ii) the second singularity occurs at

$$\lambda = 1, \tag{35}$$

or

$$m^2 \approx \Lambda^2 \tag{36}$$

and is related to final-state hadronization effects. Both soft and collinear terms are singular in this region and there are non-perturbative effects related to initial as well as final bound-state dynamics.

4 Discussion and comparison of the distributions

Let us now discuss the physics of p_\perp distributions and compare with the threshold case. In the latter case, there is a first singularity, of soft nature, closer to the origin in $\lambda = 1/2$, which can be removed by introducing the shape function. In the p_\perp case, an analogous singularity is absent, as also supported by physical intuition. In both distributions, there is a singularity in one ($\lambda = 1$ or $\omega = 1$), which cannot be removed by introducing a non-perturbative soft function. This implies that, in the p_\perp case, non-perturbative effects cannot be treated with a “shape-function” approach. One could try a different approach based on the effective theory introduced in [13] or the collinear effective theory developed in [20].

Let us note that, in general, the singularities of the functions $g_i(\omega)$ are more severe than those of the functions $g_i(\lambda)$ for $\lambda \rightarrow 1/2$ or 1. For example, $g_1(\omega)$ has a logarithmic singularity, while $g_1(\lambda)$ has an additional prefactor $1 - 2\lambda$ or $1 - \lambda$ which softens the singularity. Owing to the different singularity structure, the p_\perp -distribution is complementary to the threshold one and gives independent information about non-perturbative physics.

Finally, let us make a general field-theory remark. Threshold distributions and p_\perp -distributions have a different theoretical status. The former are completely inclusive quantities and can be computed as the imaginary part of a forward scattering amplitude: a non-perturbative computation with lattice QCD is in principle feasible [21]. This is not the case for p_\perp -distributions, which instead are true jet quantities: a separate computation of real and virtual diagrams is unavoidable and a lattice QCD computation is in principle unfeasible.

5 Conclusions

In this note we have discussed transverse momentum distributions in radiative B -decays and we have computed the next-to-leading coefficient B_1 . The structure of the logarithmic corrections is analogous to the one encountered in energy-energy correlations or shape variable distributions in e^+e^- annihilations. Owing to the different singularity structure with respect to threshold distributions, it does not seem possible to define the analogue of a shape function. An operator definition of the non-perturbative effects in this case should presumably involve a different effective theory explicitly containing the transverse degrees of freedom.

The comparison of our NLO distribution with accurate experimental data may give new and independent information about the effective size of the non-perturbative corrections of order Λ/m_B ; a recurrent problem in B -physics is indeed the separation of perturbative effects from non-perturbative ones and the estimate of the latter. The computation of the remaining next-to-leading terms — the one loop coefficient function and remainder function — is in progress and will be presented elsewhere.

Acknowledgements

One of us (U.A.) wishes to thank to S. Catani for discussions.

References

- [1] G. Parisi and R. Petronzio, Nucl. Phys. B 154, 427 (1979); G. Curci, M. Greco and Y. Srivastava, Nucl. Phys. B 159, 451 (1979); Y. Dokshitzer, D. Dyakonov and S. Troyan, Phys. Rep. 58, 269 (1980).
- [2] J. Kodaira and L. Trentadue, Phys. Lett. B 112, 66 (1982) and preprint SLAC-PUB-2934 (1982); Phys. Lett. B 123, 335 (1983); L. Trentadue Phys. Lett. B 151, 171 (1985); S. Catani, E. D'Emilio and L. Trentadue, Phys. Lett. B 211, 335 (1988).
- [3] S. Catani and L. Trentadue, Nucl. Phys. B 327, 323 (1989).
- [4] S. Catani and L. Trentadue, Nucl. Phys. B 353, 183 (1991).
- [5] S. Catani, L. Trentadue, G. Turnock and B. Webber, Nucl. Phys. B 407, 3 (1993).
- [6] S. Frixione, P. Nason, G. Ridolfi, Nucl. Phys. B 542, 311 (1999).
- [7] K. Chetyrkin, M. Misiak and M. Munz, Phys. Lett. B 400, 206 (1997); Erratum B 425, 414 (1998) and references therein.
- [8] U. Aglietti, preprint CERN-TH/2001-050, hep-ph/0103002.
- [9] D. Amati, A. Bassetto, M. Ciafaloni, G. Marchesini and G. Veneziano, Nucl. Phys. B 173, 429 (1980).
- [10] R. Akhouri and I. Rothstein, Phys. Rev. D 54, 2349 (1996).
- [11] U. Aglietti, preprint CERN-TH/2001-035, hep-ph/0102138.
- [12] G. Korchemsky and G. Sterman, Phys. Lett. B 340, 96 (1994).
- [13] U. Aglietti and G. Corbo, Phys. Lett. B 431, 166 (1998) and Int. J. Mod. Phys. A 15, 363 (2000).
- [14] U. Aglietti, Nucl. Phys. B Proc. Suppl. 96, 453 (2001).
- [15] U. Aglietti, talk given at the LEP3 conference, Rome 18-20 April 2001, to be published in the proceedings, hep-ph/0105168.
- [16] S. Catani, M. Mangano, L. Trentadue and P. Nason, Nucl. Phys. B 478, 273 (1996).
- [17] G. Altarelli, N. Cabibbo, G. Corbó, L. Maiani and G. Martinelli, Nucl. Phys. B 208, 365 (1982).
- [18] I. Bigi, M. Shifman, N. Uraltsev and A. Vainshtein, Phys. Rev. Lett. 71, 496 (1993); Int. J. Mod. Phys. A 9, 2467 (1994); A. Manohar and M. Wise, Phys. Rev. D 49, 1310 (1994); M. Neubert, Phys. Rev. D 49, 3392 and 4623 (1994); T. Mannel and M. Neubert, Phys. Rev. D 50, 2037 (1994).
- [19] U. Aglietti and G. Ricciardi, Nucl. Phys. B 587, 363 (2000).
- [20] C. Bauer, S. Fleming and M. Luke, Phys. Rev. D 63, 014006 (2001); C. Bauer, S. Fleming, D. Pirjol and W. Stewart, Phys. Rev. D 63, 114020 (2001).
- [21] U. Aglietti, M. Ciuchini, G. Corbó, E. Franco, G. Martinelli and L. Silvestrini, Phys. Lett. B 432, 411 (1998).